FEBS Open Bio 4 (2014) 301–309

journal homepage: www.elsevier.com/locate/febsopenbio

The role of autophagy in the intracellular survival of *Campylobacter concisus*

Jose A. Burgos-Portugal, Hazel M. Mitchell, Natalia Castaño-Rodríguez, Nadeem O. Kaakoush *

School of Biotechnology and Biomolecular Sciences, The University of New South Wales, Sydney, NSW 2052, Australia

ARTICLE INFO

Article history:
Received 7 January 2014
Revised 3 March 2014
Accepted 13 March 2014

Keywords:
Campylobacter concisus
Autophagy
Intracellular survival
Microscopy
Plasmid

ABSTRACT

Campylobacter concisus is an emerging pathogen that has been associated with gastrointestinal diseases. Given the importance of autophagy for the elimination of intracellular bacteria and the subversion of this process by pathogenic bacteria, we investigated the role of autophagy in _C. concisus_ intracellular survival. Gentamicin protection assays were employed to assess intracellular levels of _C. concisus_ within Caco-2 cells, following autophagy induction and inhibition. To assess the interaction between _C. concisus_ and autophagosomes, confocal microscopy, scanning electron microscopy, and transmission electron microscopy were employed. Expression levels of 84 genes involved in the autophagy process were measured using qPCR. Autophagy inhibition resulted in two- to four-fold increases in intracellular levels of _C. concisus_ within Caco-2 cells, while autophagy induction resulted in a significant reduction in intracellular levels or bacterial clearance. _C. concisus_ strains with low intracellular survival levels showed a dramatic increase in these levels upon autophagy inhibition. Confocal microscopy showed co-localization of the bacterium with autophagosomes, while transmission electron microscopy identified intracellular bacteria persisting within autophagic vesicles. Further, qPCR showed that following infection, 13 genes involved in the autophagy process were significantly regulated, and a further five showed borderline results, with an overall indication towards a dampening effect exerted by the bacterium on this process. Our data collectively indicates that while autophagy is important for the clearance of _C. concisus_, some strains may manipulate this process to benefit their intracellular survival.

1. Introduction

Autophagy is a mechanism by which cells degrade unnecessary or dysfunctional components using the lysosome [1]. It can be broadly divided into three categories: (i) macroautophagy, (ii) microautophagy, and (iii) chaperone-mediated autophagy [1], of which macroautophagy (referred to throughout as autophagy) can mediate and control bacterial clearance through lysosomal degradation. Following the induction of autophagy, the omegasome, a cup-shaped structure, is formed from the endoplasmic reticulum [2]. The isolation membrane subsequently grows and matures to engulf cytoplasmic components in a process known as elongation. The membrane then closes to form the autophagosome, a structure with a double membrane. The outer membrane of the autophagosome subsequently fuses with a lysosome to form an autolysosome [2]. Finally, lysosomal hydrolytic enzymes, including cathepsins (proteases) and lipases, degrade the intra-autophagosomal components and the inner membrane of the autophagosome [2–4].

Little is known about the intracellular survival of *Campylobacter* species and their interactions with the autophagy process of host cells. One mechanism that has been identified for *Campylobacter jejuni* is the uptake by a vacuole-like compartment [5], now known as the *Campylobacter*-containing vacuole (CCV), which diverges from the normal endocytic pathway within epithelial cells [6]. The CCV has been found to avoid delivery into lysosomes, however, its ability to do so is reliant upon the entry mechanism of *C. jejuni* [7]. More recently, Buelow et al. determined that the *Campylobacter* invasion antigen involved in Intracellular survival (CiaI), which is secreted by the type III secretion system, prevents the delivery of the CCV to lysosomes [8]. In regards to interactions with the autophagy process, Sun et al. found that mTOR (mammalian target of rapamycin) signaling, which controls autophagy, mediates *C. jejuni* induced colitis in IL-10$^{-/-}$ mice independent of T-cell

Abbreviations: CCV, Campylobacter-containing vacuole; CD, Crohn's disease; CQD, chloroquine diphosphate; Ct, threshold cycle; IBD, inflammatory bowel diseases; MOI, Multiplicity of Infection; TEM, transmission electron microscopy

* Corresponding author. Tel.: +61 (2) 9385 2057; fax: +61 (2) 9385 1483.
E-mail address: n.kaakoush@unsw.edu.au (N.O. Kaakoush).

http://dx.doi.org/10.1016/j.fob.2014.03.008
2211-5463/

activation [9]. Significantly, upon exposure to the autophagy inducer rapamycin, the authors showed that *C. jejuni* infiltration in the colon and spleen was dramatically reduced.

Campylobacter concisus is an emerging gastrointestinal pathogen, which has been associated with acute gastroenteritis, inflammatory bowel diseases (IBD) and Barrett's esophagus [10–16]. A recent study by Nielsen and colleagues reported a high incidence of *C. concisus*, almost as high as that of *C. jejuni/C. coli*, in patients with gastroenteritis from a mixed urban and rural community in Denmark [17]. Moreover, in a follow-up study [18], the authors found that 80% of *C. concisus* patients and only 32% of *C. jejuni/C. coli* patients had diarrhea for >2 weeks. Significantly, 6 months following diagnosis, while no patient previously diagnosed with *C. jejuni/C. coli* had microscopic colitis, 12% of patients infected with *C. concisus* were diagnosed with microscopic colitis, providing further support for an association between *C. concisus* and chronic intestinal diseases [14,16].

Studies on *C. concisus* have shown that the invasive potential of *C. concisus* strains isolated from chronic intestinal diseases (including IBD) are more than 500-fold higher than *C. concisus* strains isolated from acute intestinal diseases and a healthy subject [19,20]. On further investigation a plasmid containing several virulence determinants was identified that potentially could be responsible for the heterogeneity in the invasive ability of *C. concisus* strains [19]. However, more recently, in depth investigation of this plasmid has revealed that only a conserved fragment containing four genes was specific to the invasive strains, and that this fragment is more likely to be involved in intracellular survival rather than internalization into host cells [21]. Thus, in the current study, we investigated the ability of *C. concisus* to survive intracellularly in host intestinal cells through the manipulation of the autophagic system and the use of standard and modified gentamicin protection assays, confocal microscopy, scanning and transmission electron microscopy and qPCR.

2. Results and discussion

2.1. Effect of autophagy inhibition on intracellular levels of C. concisus

Following infection of intestinal epithelial cells, the intracellular levels of *C. concisus* have been shown to vary significantly between strains, with some strains having up to 500-fold more intracellular bacteria [19,20]. Numerous studies have detailed the importance of the autophagy genes *ATG16L1* and *IRGM* in combating and destroying intracellular pathogens such as *Salmonella enterica* serovar Typhimurium and *Mycobacterium tuberculosis* [22–25]. Thus, we studied the role of autophagy in governing the intracellular levels of *C. concisus* within intestinal epithelial cells. To obtain a MOI that would provide an optimal level of bacterial entry into host cells whilst not resulting in a significant amount of host cell death, we investigated the toxicity of *C. concisus* to host cells. The viability of host cells exposed to *C. concisus* at a MOI of 100, 200, 500 and 800 were determined to be 94.0 ± 0.2%, 88.2 ± 2.0%, 63.8 ± 3.3% and 50.9 ± 0.3%, respectively, when compared to a viability of 99.0 ± 0.6% for the non-infected control. We also determined the effect of atmosphere on *C. concisus* internalization by incubating the infection plate under aerobic and microaerobic conditions. This showed no significant difference in invasion levels between the two conditions. As a result, aerobic incubation of the infection plate and a MOI of 200 were chosen for the gentamicin protection assays.

The intracellular levels of *C. concisus* UNSWCD 6 h post-infection were similar to previous results obtained for this strain [19,20], with the intracellular percentage (number of internalized bacteria/number of bacteria added) of the bacterium being 0.44 ± 0.04% (Fig. 1), and the total number of intracellular bacteria being $5.1 \times 10^5 \pm 1.0 \times 10^5$ CFU ml^{-1} within the 5×10^5 host cells seeded onto the plate. This level of invasion is similar to levels of invasion observed for *C. jejuni* [26]. Upon addition of the autophagy inhibitor 3-MA at a concentration of 5 mM, the intracellular level of *C. concisus* UNSWCD increased approximately 2.2-fold. The addition of 10 mM 3-MA showed an even greater increase (approximately 3.5-fold, intracellular percentage: 1.54 ± 0.08%) in intracellular bacteria (Fig. 1). These findings were confirmed by employing alternative autophagy inhibitors, whereby the intracellular levels of *C. concisus* UNSWCD increased 2.0 and 2.8-fold upon inhibition of autophagy with 10 nM bafilomycin A-1 and 100 nM wortmannin, respectively (Fig. 1). Statistical analysis performed through a One-way ANOVA with a Dunnett's *post hoc* test showed a statistically significant increase ($P < 0.05$) for 5 and 10 mM 3-MA, 10 nM bafilomycin A-1 and 100 nM wortmannin when compared to the non-treated control.

To investigate this further, three additional *C. concisus* strains previously shown to have naturally low intracellular percentages of bacteria (ATCC 51562: 0.00048 ± 0.00016%; UNSWCS: 0.00059 ± 0.00015%) or with no invasion (BAA-1457) were employed. Interestingly, upon addition of 10 mM 3-MA, the intracellular percentages of these strains significantly increased ($P < 0.0001$) to levels observed for UNSWCD (ATCC 51562: 0.51 ± 0.06%; UNSWCS: 0.72 ± 0.14%; BAA-1457: 0.66 ± 0.09%) (Fig. 2). We then examined whether host adaptation may have a similar effect on the intracellular levels of *C. concisus* by using bacteria that internalized into host cells for the invasion assay (re-invasion). This was performed for *C. concisus* UNSWCS (0.00059 ± 0.00015%), a strain with low levels of invasion. This showed that upon re-invasion of host-adapted isolates, the intracellular percentage increased approximately 8.6-fold to 0.0051 ± 0.0009%. A further attempt at re-invasion of internalized isolates did not alter the intracellular percentage (0.0045 ± 0.0011%), and a third re-invasion resulted in isolates with gentamicin resistance. These findings would suggest that the autophagy process is one of the primary regulators of intracellular levels of *C. concisus* strains with low invasion percentages.

The compounds 3-MA and wortmannin act by blocking phosphotidyl-inositol-3-kinase activity, while bafilomycin A-1 inhibits vacuolor ATPase all of which result in autophagy inhibition [27].

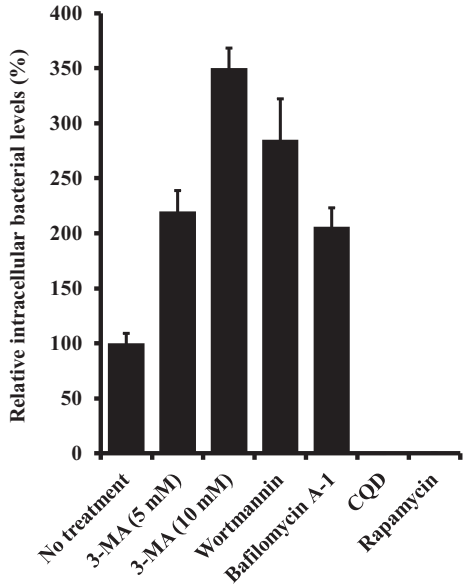

Fig. 1. Relative intracellular percentage of *C. concisus* UNSWCD following autophagy inhibition and induction. Errors are presented as Standard Error of the Mean (SEM) based on a minimum of four biological replicates. 3-MA: 3-methyladenine; CQD: 50 μM chloroquine diphosphate; rapamycin: 200 nM rapamycin.

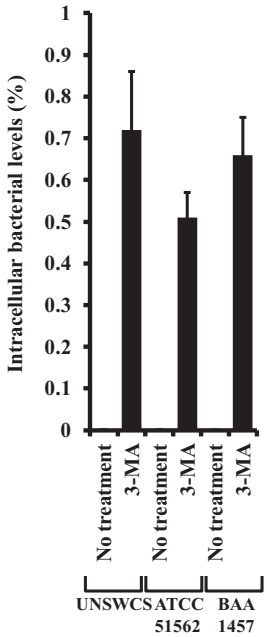

Fig. 2. Intracellular percentage of *C. concisus* UNSWCS, ATCC 51562 and BAA-1457 following autophagy inhibition. Errors are presented as Standard Error of the Mean (SEM) based on a minimum of four biological replicates. 3-MA: 10 mM 3-methyladenine.

Given the importance of autophagy in eliminating intracellular pathogens, it would be expected that if this pathway is involved in the pathogenesis of *C. concisus*, inhibition of this process would result in increased levels of intracellular *C. concisus*. Strikingly, while the strain with high invasion showed a 3.5-fold increase, strains with low or no invasion into host cells showed a dramatic increase (>1000-fold) in intracellular levels upon inhibition of autophagy. In support of this finding, a study by Lapaquette et al. showed that siRNA-mediated knock down of *ATG16L1* or *IRGM* in HeLa cells resulted in increased proliferation of adherent and invasive *Escherichia coli* [22].

2.2. Effect of autophagy induction on intracellular levels of C. concisus

Addition of the autophagy inducer rapamycin (200 nM) and the autophagy modulator CQD (50 μM) resulted in significant decreases ($P < 0.0001$) in intracellular levels of *C. concisus* UNSWCD, with the intracellular percentage being 0.0007 ± 0.0001% and 0%, respectively (Fig. 1). Rapamycin, is a known inducer of autophagy through its action on mTOR. Induction of autophagy by this compound resulted in the highly invasive strain UNSWCD having intracellular levels similar to those of the low invasive strains ATCC 51562 and UNSWCS. The effect on *C. jejuni* intracellular survival is less pronounced, with a 75% reduction in survival being seen in murine embryonic fibroblasts and HT-29 cells induced to undergo autophagy with rapamycin [28]. A similar concentration of rapamycin used in a study by Yuan et al. on *Pseudomonas aeruginosa* yielded total bacterial clearance [29]. Moreover, Wang et al. showed rapamycin could inhibit the multiplication of *Helicobacter pylori* at 6 and 12 h post infection of THP-1 cells [30].

CQD plays a more complex role in the cell having been associated with stimulation of autophagosome formation. It has also been shown to accumulate inside lysosomes leading to inhibition of lysosomal enzymes [31]. Addition of CQD resulted in complete bacterial clearance, a finding that is supported by a study by Oelschlaegear et al. which found a reduction in the intracellular survival of *C. jejuni*, *E. coli*, *Citrobacter freundii* and *S.* Typhimurium upon addition of CQD [32]. The authors of this study suggested that the most likely cause of this was the intracellular accumulation of CQD to bactericidal concentrations [32]. To determine if this was the case we investigated the effect of CQD on the viability of *C. concisus* UNSWCD. While this compound resulted in a decrease in bacterial numbers of up to 1.2 log (25 μM CQD), 1.7 log (50 μM CQD) and 2.8 log (100 μM CQD), it did not result in bacterial clearance. Moreover, while the viability of the host cells exposed to 50 μM CQD for 14 h significantly decreased to 75.2 ± 2.0% when compared to the non-induced control (98.8 ± 0.6%), this could not fully explain the lack of intracellular bacteria in Caco-2 cells exposed to CQD. To investigate this further, we visualized the Caco-2 cells exposed to 50 μM CQD using scanning electron microscopy, and found cellular protrusions (blebs) on the apical membrane surface (Fig. 3B, C) that were not present in the negative control (Fig. 3A). The regions surrounding these protrusions showed a significant decrease in microvilli abundance (Fig. 3B, C). These findings are supported by a study by Fan et al. which reported exposure to high concentrations of CQD to result in vacuolation and blebbing in A549 lung cancer cells [33]. Thus, although cellular alterations and toxicity as a consequence of CQD exposure will result in a significant decrease in intracellular levels of *C. concisus*, the effects that CQD exerts on autophagy are also likely to be involved in the complete bacterial clearance observed.

These results collectively indicate that the host autophagy process controls the intracellular levels of *C. concisus*, and that some strains of this bacterium have the ability to overcome or manipulate this process. To confirm our findings, we then investigated this phenomenon further by visualizing *C. concisus* infection through confocal microscopy and transmission electron microscopy.

2.3. Co-localization of C. concisus with autophagosomes

Autophagosomes were detected through the presence of LC3B in Caco-2 cells distributed within the cytoplasm and near the membrane regions of the cells (Fig. 4A), indicating that autophagy is an active process that normally occurs within Caco-2 cells. Inhibition of the autophagy process using 3-MA at 5 and 10 mM resulted in downregulation of autophagosome formation in Caco-2 cells (Fig. S1). In contrast, the density of LC3B detected following induction of autophagosomes with 50 μM CQD was higher than that observed in the Caco-2 cells without chemical treatment (Fig. S1), consistent with the activity of these compounds. Following infection of Caco-2 cells with *C. concisus* UNSWCD, the bacterium was found to co-localize with LC3B (Fig. 4B–I). Moreover, some cells were found to be hyperinfected by *C. concisus* UNSWCD (Fig. 4F, J). Calculation of the co-localization coefficient for the *C. concisus* antibody and the LC3B antibody showed the coefficient to range from 0.54 to 0.90, indicating that significant co-localization between the two antibodies existed. The fact that *C. concisus* UNSWCD interacts with the autophagosome, provides further evidence that autophagy is involved in the intracellular survival of *C. concisus* within host cells, and raises the possibility that *C. concisus* could employ autophagy to survive intracellularly. A similar observation has been made with *C. jejuni*, with the bacterium co-localizing with GFP-LC3-labeled structures consistent with autophagosomes [28]. In a recent study, Lam et al. reported that *Listeria monocytogenes* co-localizes with LC3 [34], a finding that led them to suggest that this co-localization gives rise to spacious *Listeria*-containing phagosomes, membrane-bound compartments that harbor slow-growing bacteria associated with persistent infection [34].

Further, the association between *C. concisus* infection and the autophagy process was visualized in more detail using TEM. Observation of the TEM images showed the bacterium to be densely stained and to have spiral shaped morphology (Fig. 5A, B). The

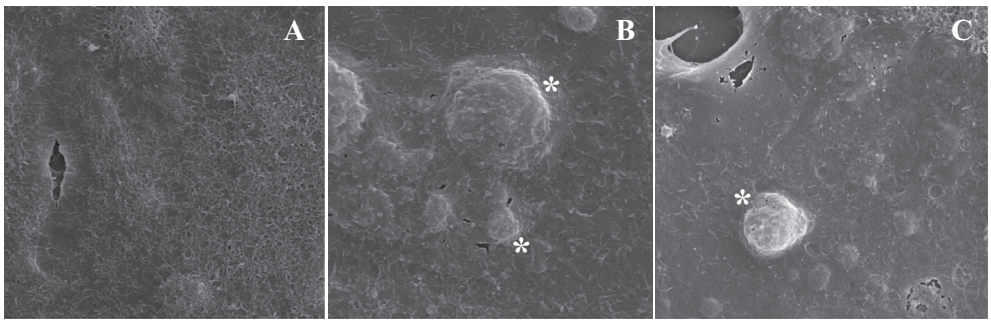

Fig. 3. Scanning electron microscopy images of Caco-2 cells without (A) and with chloroquine diphosphate treatment (B, C). Following treatment of Caco-2 cells with 50 μM CQD, cellular protrusions/blebs (indicated by an asterisk) were induced on the apical membrane surface of Caco-2 cells.

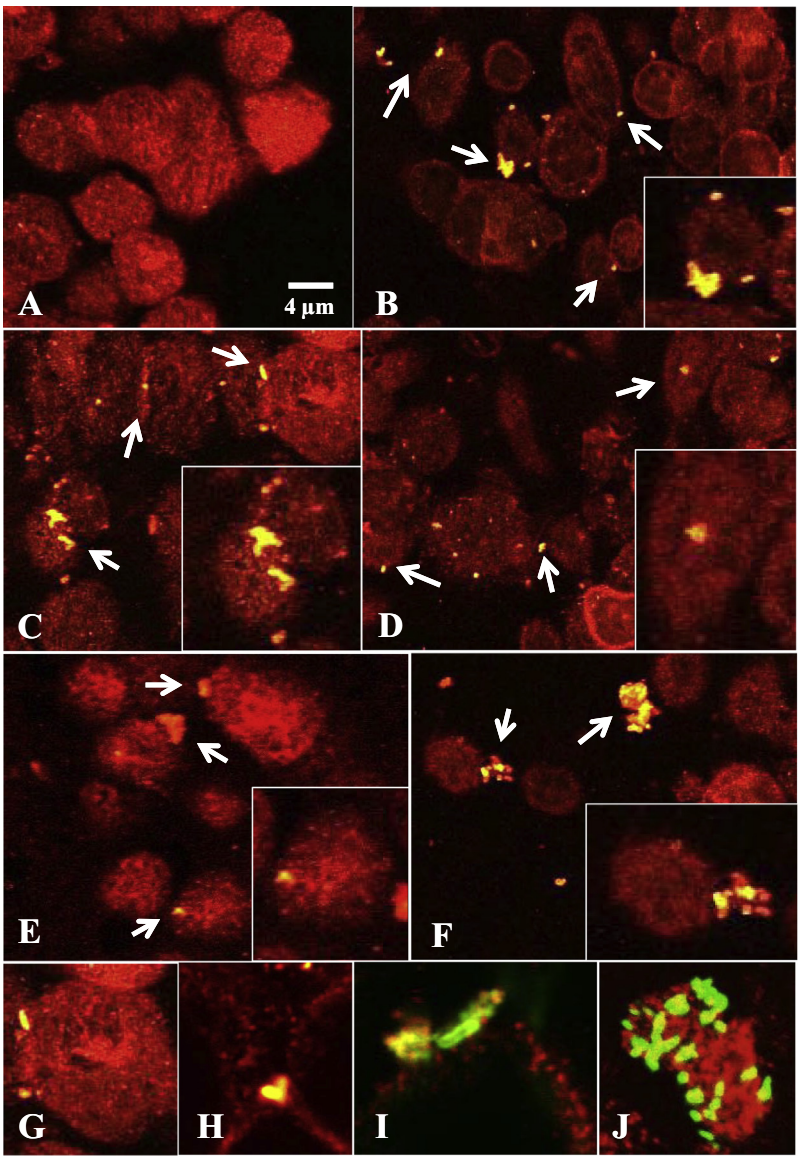

Fig. 4. Visualization of the co-localization of *C. concisus* with autophagosomes using confocal microscopy. (A) Untreated Caco-2 cells, (B–J) Caco-2 cells infected with *C. concisus* UNSWCD. LC3B was stained in red, *C. concisus* was stained in green. *C. concisus* UNSWCD was found to aggregate and adhere to Caco-2 cells, internalize into Caco-2 cells, and co-localize with the LC3B antibody (B–J).

dimensions of *C. concisus* UNSWCD were 4 μm long × 0.5 μm wide (Fig. 5A, B), which is consistent with previous reports on the size of the bacterium. An outer layer around the bacterium was identified (Fig. 5A, B), that may correspond to the formation of a capsule as has been shown in *C. jejuni* [35]. TEM images of Caco-2 cells not infected with the bacterium showed typical characteristics such as microvilli on the apical membrane surface and vacuolar compartments with no darkly stained material between the apical

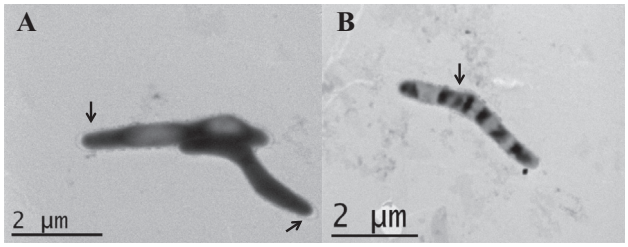

Fig. 5. Transmission electron microscopy images of *Campylobacter concisus* UNSWCD. (A) The bacterium is densely stained, showing spiral shaped morphology. (B) The dimensions of *C. concisus* UNSWCD appears to be 4 μm long × 0.5 μm wide. There appears to be an outer layer forming around the bacterium indicated by arrows.

membrane surface and the nucleus (Fig. 6A). At the initial stages of infection with *C. concisus* UNSWCD, Caco-2 cells appeared more rounded than non-infected cells (Fig. 6B). Infected cells contained a higher number of vacuoles (Fig. 6B, C), lysosomes showing a one layered membrane encapsulating dense granular material (Fig. 6D), and internalized bacteria (densely stained) in close association with mitochondria (Fig. 6E). Moreover, some internalized *C. concisus* UNSWCD cells were found to be inside a vacuole (Fig. 6F), most likely to be a *Campylobacter*-containing vacuole [6]. This vacuole compartment may allow *C. concisus* UNSWCD to persist intracellularly, as this CCV was found closer to the basolateral end. Such a defensive mechanism to evade lysosomal degradation has been previously identified for *C. jejuni* [7]. More recently, Bouwman et al. have demonstrated that intracellular *C. jejuni* can reside in membrane-bound CD63-positive cellular compartments [36]. Thus, it would be of interest to determine if compartments containing *C. concisus* were also CD63 positive.

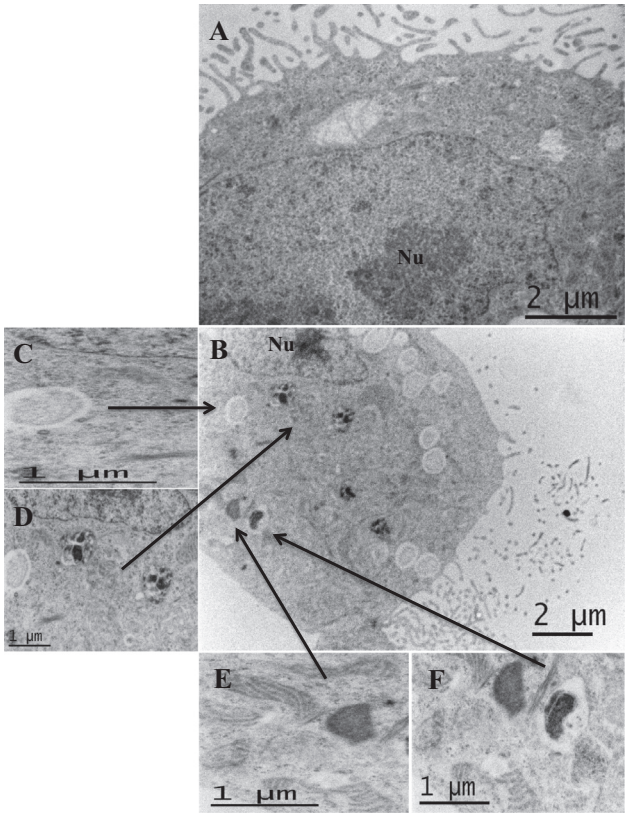

Fig. 6. Transmission electron microscopy images of Caco-2 cells reflecting the initial stages of *Campylobacter concisus* UNSWCD infection. (A) Image shows characteristics of a Caco-2 cell. Microvilli are observed on the apical membrane surface, vacuolar compartments with no cellular material can be found between the apical membrane surface and the nucleus (Nu). (B) Image of a Caco-2 cell infected by *C. concisus* UNSWCD. Notable characteristics include lysosomal compartments, vacuoles and a *Campylobacter*-containing vacuole. (C) High magnification image of a Caco-2 cell vacuole. A granular compartment can be seen inside the vacuole. (D) High magnification image of two lysosomes showing a one layered membrane encapsulating dense granular material. (E) High magnification image of Caco-2 cell mitochondria and a densely stained bacterium. The mitochondria show a clear cristae lining and appear close to a bacterial cell, which may suggest a possible association between mitochondria and *C. concisus* UNSWCD in the formation and maturation of autophagosomes. (F) *C. concisus* UNSWCD within Caco-2 cells inside a *Campylobacter*-containing vacuole.

C. concisus UNSWCD cells found in close proximity to mitochondria were encapsulated by a fine layer (Fig. 7A, B), which could be indicative of early stage phagosome formation in Caco-2 cells. Filament arrangements were also identified near the bacterium (Fig. 7B, C). *C. concisus* UNSWCD were found to associate with autophagosomes showing a fine double membrane, one of their distinct characteristics (Fig. 7D). They were also found in close proximity to intermediary phagosomes (Fig. 7E), and in fusion with larger phagosomes containing both a vacuole compartment and an intermediary phagosome (Fig. 7F, G). Moreover, *C. concisus* UNSWCD can be found inside autophagolysosomes with dense granular material (Fig. 7H, I), in some cases its spiral morphology being still detectable (Fig. 7I).

It is apparent through the evidence provided based on both confocal microscopy and TEM that *C. concisus* internalization is associated with the autophagy process, suggesting the bacterium may manipulate the process to persist within epithelial cells.

2.4. Modulation in the expression of genes involved in autophagy by C. concisus

Given the role of autophagy in modulating the intracellular levels of *C. concisus* and possible evasion of some strains of autophagy-mediated killing, we analyzed the effect of *C. concisus* UNSWCD infection on the gene expression of 84 genes involved in autophagy. Out of the 84 genes analyzed, three genes were found to be significantly upregulated and 16 genes were found to be downregulated (10 significant, 6 borderline) (Table 1, Table S1). Interestingly, the collective level of regulation of these genes suggested that *C. concisus* exerts a weak inhibitory/dampening effect on the autophagy process (approximately 80% of normal levels), suggesting that the bacterium exerts some level of manipulation on the process. Moreover, the downregulation of both *FADD* (associated with caspase 8 [37]) and *BAX* (accelerates apoptosis [38]), suggests that host cells infected with *C. concisus* downregulate autophagy-related apoptosis.

Genes involved in the regulation of autophagy by the host cell appeared to be downregulated through the effect on the genes *IGF1*, *MAPK14* and *HDAC1* (Table 1). Both *IGF1* and *MAPK14* have been shown to be inhibitors of autophagy [39,40]. However, this downregulation is not limited to inhibitors of autophagy. HDAC1 is a histone deacetylase that has also been shown to induce autophagic gene expression in mice [41], indicating that host regulation of the autophagy process as a whole is affected by the bacterium.

In mammalian cells, autophagy-related proteins can be divided into five subgroups: the ULK1 protein-kinase complex, the ATG9-WIPI complex, the Vps34-beclin1 class III phosphoinositide 3 (PI3)-kinase complex, the Atg12 conjugation system, and the LC3 conjugation system [2]. *Atg9b* and *WIPI1*, two components of the ATG9-WIPI complex, which is involved in the nucleation of autophagic vesicles [2], were shown to be downregulated upon infection with *C. concisus* (Table 1). Moreover, AMBRA1, a positive regulator of beclin1-regulated autophagy through its association with the Vps34-beclin1 class III PI3-kinase complex, was also downregulated. This complex has also been associated with

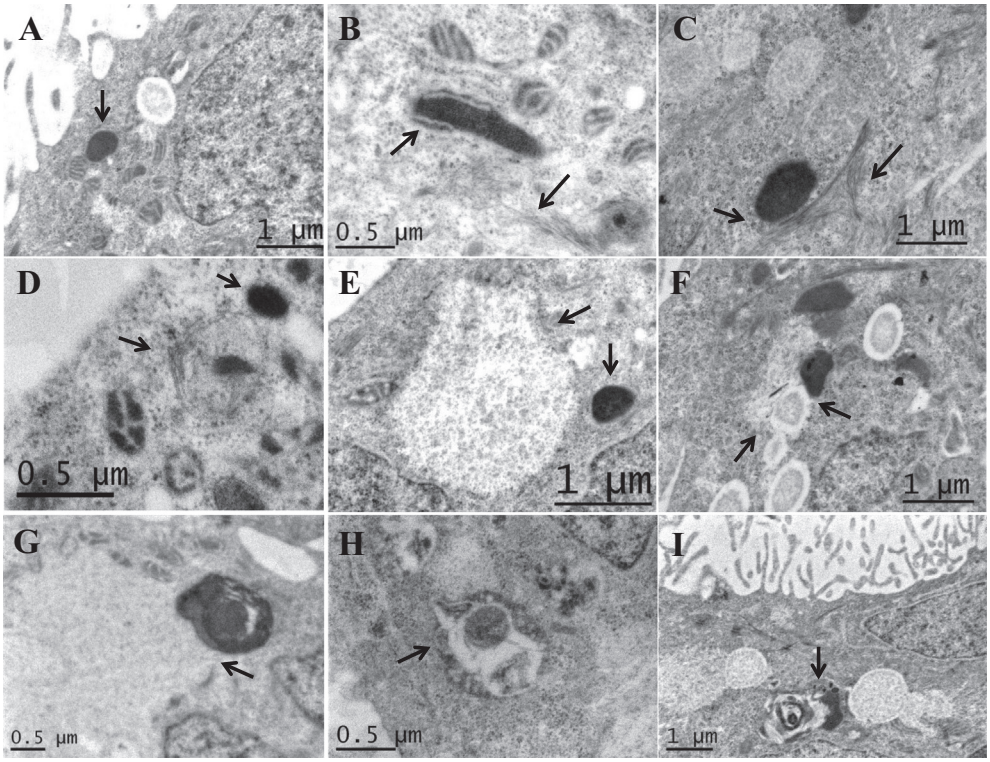

Fig. 7. Visualization of the internalization of *C. concisus* into Caco-2 cells using transmission electron microscopy. (A) *C. concisus* UNSWCD invading inside Caco-2 cells shown in cross section measuring 0.5 µm wide. The bacterial cell appears to be in close proximity to a mitochondrion with a fine layer surrounding them. (B) A membrane forms around internalized *C. concisus* UNSWCD. A fine layer surrounds the bacterium alongside mitochondria and could be indicative of early stage phagosome formation in Caco-2 cells. (C) The appearance of fine filament arrangements close to the bacterium. (D) *C. concisus* UNSWCD associated with an autophagosome showing a double membrane. (E) *C. concisus* UNSWCD shown in cross section (0.5 µm wide) in close proximity to an intermediary phagosome. The bacterium appears to be within a vacuole. (F) *C. concisus* UNSWCD shown in cross section (0.5 µm wide). The bacterium is shown in close proximity with a vacuole compartment forming one large phagosome. (G) High magnification image of the bacterium fusing with a vacuole compartment. (H) *C. concisus* UNSWCD (0.5 µm wide) observed inside an autophagolysosome containing dense granular material. (I) A Caco-2 cell showing a clear apical membrane surface with microvilli. *C. concisus* UNSWCD which has maintained its spiral morphology is visualised inside an autophagolysosome.

Table 1
Genes within the autophagy pathway that are regulated upon infection with *C. concisus* UNSWCD. Three biological replicates from each of the non-infected and infected cells were analyzed.

Gene	Gene name	Refseq	Fold change	*P*-value	95% CI
BID	BH3 interacting domain death agonist	NM_001196	1.0876	0.025435	(1.04, 1.14)
CDKN2A	Cyclin-dependent kinase inhibitor 2A	NM_000077	1.0926	0.025666	(1.04, 1.15)
MAP1LC3B	Microtubule-associated protein 1 light chain 3 beta	NM_022818	1.2697	0.018016	(1.12, 1.42)
AMBRA1	Autophagy/beclin-1 regulator 1	NM_017749	0.7142	0.016645	(0.59, 0.84)
ATG4B	ATG4 autophagy related 4 homolog B	NM_178326	0.7888	0.0155	(0.69, 0.88)
ATG7	ATG7 autophagy related 7 homolog	NM_006395	0.8017	0.012916	(0.72, 0.88)
ATG9B	ATG9 autophagy related 9 homolog B	NM_173681	0.7497	0.034192	(0.60, 0.90)
BAX	BCL2-associated X protein	NM_004324	0.8035	0.030812	(0.70, 0.91)
CTSD	Cathepsin D	NM_001909	0.8572	0.011508	(0.80, 0.91)
CTSS	Cathepsin S	NM_004079	0.6649	0.059751	(0.45, 0.88)
FADD	Fas (TNFRSF6)-associated via death domain	NM_003824	0.6378	0.051529	(0.46, 0.82)
GABARAPL1	GABA(A) receptor-associated protein like 1	NM_031412	0.9124	0.021973	(0.87, 0.96)
HDAC1	Histone deacetylase 1	NM_004964	0.8204	0.002512	(0.78, 0.86)
HSPA8	Heat shock 70 kDa protein 8	NM_006597	0.798	0.019944	(0.70, 0.89)
IGF1	Insulin-like growth factor 1	NM_000618	0.4878	0.088337	(0.15, 0.83)
LAMP1	Lysosomal-associated membrane protein 1	NM_005561	0.8166	0.067864	(0.70, 0.93)
MAPK14	Mitogen-activated protein kinase 14	NM_001315	0.8875	0.064372	(0.81, 0.97)
TGFB1	Transforming growth factor, beta 1	NM_000660	0.7209	0.029435	(0.57, 0.88)
WIPI1	WD repeat domain, phosphoinositide interacting 1	NM_017983	0.8357	0.057777	(0.72, 0.95)

autophagosome nucleation [2]. The LC3 conjugation system was also affected by *C. concisus* infection, through the downregulation of both *Atg4B* and *Atg7* (Table 1). ATG4B and ATG7 are involved in the conversion of proLC3 to LC3-I to LC3-II and back to LC3-I, a process that regulates autophagosome maturation and fusion of autophagosomes with lysosomes [2], suggesting that infection leads to inhibition or dampening of these processes. Notably, *MAP1LC3B* was significantly upregulated, with fold level changes

correlating to the decreases in *ATG4B* and *ATG7* transcription (Table 1). The upregulation of *MAP1LC3B* is considered a marker of autophagy inhibition.

Further evidence to support the dampening effect on autophagosome-lysosome fusion comes from the downregulation of *LAMP1*, *CTSD* and *CTSS* (Table 1). *LAMP1*, also known as CD107a (Cluster of Differentiation 107a), is a critical lysosomal adaptor protein that is involved in the interaction and fusion of the lysosomes with various cell components [2,42]. Moreover, deficiencies in both cathepsin D (CTSD) and cathepsin S (CTSS) have been shown to result in accumulation of autophagosomes and impairment of autolysosome degradation [43,44]. Interestingly, in a previous study investigating the changes in protein expression upon infection with *C. concisus*, cathepsin D was also identified to be downregulated [19], indicating that these changes are reflected at the protein level. Collectively, these results show a dampening effect on autophagosome maturation and autophagosome-lysosome fusion, suggesting *C. concisus* may utilize autophagic vesicles that have not matured for its intracellular survival. Similarly, the closely-related pathogen *C. jejuni* forms the CCV that associates with the early endosomal markers Rab 4 and 7 to escape lysosomal degradation [7].

3. Conclusions

This study has shown for the first time that autophagy plays an important role in modulating the intracellular levels of *C. concisus* strains. Moreover, our results would suggest that differences in the intracellular levels of *C. concisus* strains are associated with the ability of these strains to interact with the autophagy process, with some strains being able to evade destruction by autophagy more efficiently than others. Previous studies by our group would suggest that the increased ability of *C. concisus* to survive intracellularly might be due to four conserved genes on a plasmid within some strains [19,21]. Thus, it is plausible that these *C. concisus* genes may interact with the host autophagy process to enhance the intracellular survival of this bacterium. Interestingly, *C. concisus* has been associated with Crohn's disease (CD) [16,23]. Given that polymorphisms in the autophagy genes *ATG16L1* and *IRGM* are known to confer susceptibility to CD [24,45] and that an increased number of autophagosomes are observed in CD patients [46], further investigation of the role of *C. concisus* as an initiator of this disease should be the focus of future studies.

4. Materials and methods

4.1. Bacterial strains and growth

The four *C. concisus* strains UNSWCD, UNSWCS, ATCC 51562 and BAA-1457 were used in this study. UNSWCD and UNSWCS were isolated as part of previous studies [16,20] which were approved by the Research Ethics Committees of the University of New South Wales and the South East Sydney Area Health Service-Eastern Section, Sydney (Ethics No.: 06/164). ATCC 51562 and BAA-1457 were purchased from the American Type Culture Collection. *C. concisus* strains were grown on Horse Blood Agar (HBA) plates [Blood Agar Base No. 2 supplemented with 6% defibrinated horse blood (Oxoid)], and incubated at 37 °C under microaerobic conditions with H_2 [generated using *Campylobacter* Gas Generating Kits (Cat. #. BR0056A, Oxoid; Adelaide, SA, Australia)] for 48 h.

4.2. Cell culture

The human intestinal epithelial cell line Caco-2 (American Type Culture Collection; HTB-37) was used in this study. Cells were grown in 10 ml cell culture media comprised of Minimum Essential Medium (MEM) (Life technologies; Mulgrave, VIC, Australia) supplemented with 10% FBS, 1 mM sodium pyruvate, 0.1 mM non-essential amino acids, 2.25 mg l^{-1} sodium bicarbonate and 100 μg ml^{-1} penicillin and streptomycin (Life technologies) in 25 cm^2 tissue culture flasks (In Vitro Technologies; Noble Park, VIC, Australia) at 37 °C with 5% CO_2. Cell viability was determined by performing a cell count on the trypsinized cells using a haemocytometer and 0.4% trypan blue (Sigma Aldrich; Castle Hill, NSW, Australia).

4.3. Determination of intracellular levels of C. concisus using gentamicin protection assays

Cells were seeded at a concentration of 5×10^5 cells ml^{-1} into 24-well plates and incubated for 2 days at 37 °C with 5% CO_2. Prior to seeding, the wells were coated with 1 ml collagen (0.338 mg ml^{-1}) and incubated for 20 min at 37 °C with 5% CO_2. Monolayers were infected with the bacteria at a Multiplicity of Infection (MOI) of 200. Following the addition of the bacteria, the 24-well plates were centrifuged at 232*g* for 5 min to promote bacterial-human cell contact. Infected monolayers were then co-incubated with the bacteria for 6 h at 37 °C with 5% CO_2 to allow adherence and invasion to occur. Invasion assays were performed as previously described by Man et al. [20]. To examine the effect of incubation conditions on invasion levels of *C. concisus*, infected monolayers were either incubated for 6 h at 5% CO_2 (aerobic) or under microaerobic conditions with H_2 (generated using *Campylobacter* Gas Generating Kits). To examine the effect of autophagy inhibition on intracellular levels of *C. concisus*, 5 mM or 10 mM 3-methyladenine (3-MA), 10 nM bafilomycin A-1 or 100 nM wortmannin (Sigma Aldrich) were added to the monolayer 1 h prior to the addition of the bacteria. To examine the effect of autophagy induction on intracellular levels of *C. concisus*, rapamycin or chloroquine diphosphate (CQD) (Sigma Aldrich) were added to the monolayer at concentrations of 200 nM and 50 μM, respectively, 14 h prior to commencement of the assay. Statistical analyses were performed using a one-way or two-way ANOVA with a *post hoc* Dunnett's test employing GraphPad Prism version 5.0 (GraphPad Software; San Diego, CA, USA).

4.4. Determination of the effect of chloroquine diphosphate on the ability of Caco-2 cells to exocytose C. concisus

To examine the effect of CQD on the ability of Caco-2 cells to exocytose *C. concisus*, Caco-2 cells were seeded as previously described, and infected with *C. concisus* UNSWCD at a MOI of 200 for 6 h. Following the incubation period, monolayers were washed with media without antibiotics three times and exposed to 200 μg ml^{-1} gentamicin for 1 h to remove any extracellular bacteria. After gentamicin treatment, the cells were washed with media without antibiotics three times, and 50 μM CQD was added to the respective wells and incubated for 1 h. The supernatant was collected and extracellular bacteria were quantified using a drop plate count method on HBA plates. The intracellular bacteria were also quantified.

4.5. Determination of the effect of chloroquine diphosphate on C. concisus viability

C. concisus was grown in a broth medium consisting of Brain heart infusion (BHI) (Oxoid), 10% FBS, and CQD at concentrations of 0 μM, 25 μM, 50 μM, and 100 μM for 24 h under microaerobic conditions. Bacterial viability was quantified by serial dilution with PBS on HBA plates using a drop plate count method.

4.6. Detection of autophagosomes and bacterial co-localization through confocal microscopy

Caco-2 cells were grown at 37 °C with 5% CO_2 on 13 mm poly-L-lysine coated glass cover slips (Thermoline Scientific; Wetherill Park, NSW, Australia) in 24-well plates at a concentration of 5×10^5 cells per well for 48 h. Cells were infected with *C. concisus* UNSWCD at a MOI of 200 for 6 h. As a positive control for autophagosome formation, Caco-2 cells were treated with 50 μM CQD for 14 h prior to commencing the assay. To investigate autophagy inhibition, 5 mM and 10 mM concentrations of 3-MA were used. Caco-2 cells were fixed in 3.7% formaldehyde and cells were then permeabilized using 0.2% Triton-X 100 in PBS for 15 min at room temperature. Autophagosomes were labelled with anti-LC3B mouse antibody (0.5 μg ml^{-1}) (Sigma Aldrich) and *C. concisus* UNSWCD was labelled with anti-*C. concisus* rabbit sera (1:30) and incubated at room temperature for 1 h. The secondary antibodies anti-mouse antibody Alexa Fluor 594 (5 μg ml^{-1}) and anti-rabbit antibody Alexa Fluor 488 (5 μg ml^{-1}) (Life technologies) were added for 1 h at room temperature. Specimens were visualized using an Olympus FluoviewTM FV1000 confocal laser scanning microscope (Olympus; North Ryde, NSW, Australia). Co-localization was measured by calculating Pearson's correlation coefficients (RTotal and Rcoloc values >0.5 are indicative of co-localization) using the Fiji software (http://fiji.sc/Fiji).

4.7. Detection of membrane alterations by scanning electron microscopy

Caco-2 cells were grown at 37 °C with 5% CO_2 on 13 mm poly-L-lysine coated glass cover slips in 24-well plates at a concentration of 5×10^5 cells per well for 48 h. Cells were infected with *C. concisus* UNSWCD at a MOI of 200 for 6 h and samples were visualized on a Hitachi S3400-X Scanning Electron Microscope (Hitachi High-Technologies Corporation; Tokyo, Japan) as previously described [20]. As a positive control of autophagosome formation, 50 μM CQD was added to the Caco-2 cells 14 h prior to commencing the assay.

4.8. Detection of intracellular bacteria and autophagosomes by transmission electron microscopy

Transmission electron microscopy (TEM) was employed to visualize and quantify intracellular *C. concisus* and determine their interactions with autophagosomes. Caco-2 cells were grown at 37 °C with 5% CO_2 on 6-well plates at a concentration of 1×10^6 cells per well for 48 h. Cells were infected with *C. concisus* UNSWCD at a MOI of 200 for 6 h and then collected using a cell scraper. As a positive control of autophagosome formation, 50 μM of CDQ or 200 nM rapamycin were added to the Caco-2 cell culture media 14 h prior to commencing the assay. Samples were embedded in London Resin (LR) White (ProSciTech; Kirwan, QLD, Australia) and sectioned to ultra-thin levels of 70 nm using an Ultramicrotome EM UC6 (Leica Microsystems; North Ryde, NSW, Australia). Each grid was then stained via a positive staining method using 8% uranyl acetate and Reynold's lead citrate (ProSciTech). Specimens were viewed using a JEOL JEM-1400 Transmission electron microscope (JEOL USA Inc.; Peabody, MA, USA). The samples were analyzed at an acceleration voltage of 100 kV and 55 μA at calibrated magnifications.

4.9. Quantitative PCR for analysis of genes within the autophagy pathway

Caco-2 cells were grown at 37 °C with 5% CO_2 on 6-well plates at a concentration of 1×10^6 cells per well for 48 h. Cells were then infected with *C. concisus* UNSWCD at a MOI of 200 for 6 h. RNA was extracted from the cells using the Isolate I RNA extraction kit (Bioline; Alexandria, NSW, Australia). cDNA was prepared using a RT^2 First strand cDNA synthesis kit according to the manufacturer's instructions (Qiagen; Chadstone Centre, VIC, Australia). The cDNA samples were then mixed with the RT^2 SYBR Green Fast Master mix (Qiagen), and aliquoted in equal volumes of 20 μl to each well of the Human Autophagy RT^2 Profiler™ (PAHS-084) array (Qiagen), which targets 84 genes related to the autophagy pathway. Transcription profiles were obtained from three independent experiments of *C. concisus* UNSWCD infected (test) and non-infected (control) samples. The threshold cycle (Ct) of each gene was determined, and subsequently analyzed by the RT^2 Profiler PCR Array data analysis software. ΔΔCt values were determined following normalization of the data using a relevant combination of housekeeping genes provided within the array. Statistically significant values were defined as $P < 0.05$.

Author contribution statement

HMM and NOK conceived the idea; JAB-P performed the gentamicin protection assays and all microscopy experiments; NCR and JAB-P performed the qPCR experiments; JAB-P, NOK, HMM and NCR analysed the results; NOK, JAB-P, HMM and NCR drafted the manuscript.

Acknowledgements

The authors would like to thank Jennifer Norman from the Electron Microscopy unit, UNSW for her technical assistance.

NOK is supported by an Early Career fellowship from the National Health and Medical Research, Australia. NOK and HMM acknowledge support from the University of New South Wales.

No conflicts of interest exist.

Appendix A. Supplementary data

Supplementary data associated with this article can be found, in the online version, at http://dx.doi.org/10.1016/j.fob.2014.03.008.

References

[1] Deretic, V. and Levine, B. (2009) Autophagy, immunity, and microbial adaptations. Cell Host Microbe 5, 527–549.
[2] Tanida, I. (2011) Autophagosome formation and molecular mechanism of autophagy. Antioxid. Redox Signal. 14, 2201–2214.
[3] Choi, A.M., Ryter, S.W. and Levine, B. (2013) Autophagy in human health and disease. New Engl. J. Med. 368, 651–662.
[4] Mehrpour, M., Esclatine, A., Beau, I. and Codogno, P. (2010) Overview of macroautophagy regulation in mammalian cells. Cell Res. 20, 748–762.
[5] De Melo, M.A., Gabbiani, G. and Pechere, J.C. (1989) Cellular events and intracellular survival of *Campylobacter jejuni* during infection of HEp-2 cells. Infect. Immun. 57, 2214–2222.
[6] Konkel, M.E., Hayes, S.F., Joens, L.A. and Cieplak Jr., W. (1992) Characteristics of the internalization and intracellular survival of *Campylobacter jejuni* in human epithelial cell cultures. Microb. Pathog. 13, 357–370.
[7] Watson, R.O. and Galan, J.E. (2008) *Campylobacter jejuni* survives within epithelial cells by avoiding delivery to lysosomes. PLoS Pathog. 4, e14.
[8] Buelow, D.R., Christensen, J.E., Neal-McKinney, J.M. and Konkel, M.E. (2011) *Campylobacter jejuni* survival within human epithelial cells is enhanced by the secreted protein CiaI. Mol. Microbiol. 80, 1296–1312.
[9] Sun, X., Threadgill, D. and Jobin, C. (2012) *Campylobacter jejuni* induces colitis through activation of mammalian target of rapamycin signaling. Gastroenterology 142, 86–95.
[10] Blackett, K.L., Siddhi, S.S., Cleary, S., Steed, H., Miller, M.H., Macfarlane, S., Macfarlane, G.T. and Dillon, J.F. (2013) Oesophageal bacterial biofilm changes in gastro-oesophageal reflux disease, Barrett's and oesophageal carcinoma: association or causality? Aliment. Pharmacol. Ther. 37, 1084–1092.
[11] Lastovica, A.J. (2009) Clinical relevance of *Campylobacter concisus* isolated from pediatric patients. J. Clin. Microbiol. 47, 2360.
[12] Macfarlane, S., Furrie, E., Macfarlane, G.T. and Dillon, J.F. (2007) Microbial colonization of the upper gastrointestinal tract in patients with Barrett's esophagus. Clin. Infect. Dis. 45, 29–38.

[13] Mahendran, V., Riordan, S.M., Grimm, M.C., Tran, T.A., Major, J., Kaakoush, N.O., Mitchell, H. and Zhang, L. (2011) Prevalence of *Campylobacter* species in adult Crohn's disease and the preferential colonization sites of *Campylobacter* species in the human intestine. PLoS One 6, e25417.
[14] Man, S.M., Zhang, L., Day, A.S., Leach, S.T., Lemberg, D.A. and Mitchell, H. (2010) *Campylobacter concisus* and other *Campylobacter* species in children with newly diagnosed Crohn's disease. Inflamm. Bowel Dis. 16, 1008–1016.
[15] Mukhopadhya, I., Thomson, J.M., Hansen, R., Berry, S.H., El-Omar, E.M. and Hold, G.L. (2011) Detection of *Campylobacter concisus* and other *Campylobacter* species in colonic biopsies from adults with ulcerative colitis. PLoS One 6, e21490.
[16] Zhang, L., Man, S.M., Day, A.S., Leach, S.T., Lemberg, D.A., Dutt, S., Stormon, M., Otley, A., O'Loughlin, E.V., Magoffin, A., Ng, P.H. and Mitchell, H. (2009) Detection and isolation of *Campylobacter* species other than *C. jejuni* from children with Crohn's disease. J. Clin. Microbiol. 47, 453–455.
[17] Nielsen, H.L., Ejlertsen, T., Engberg, J. and Nielsen, H. (2013) High incidence of *Campylobacter concisus* in gastroenteritis in North Jutland, Denmark: a population-based study. Clin. Microbiol. Infect. 19, 445–450.
[18] Nielsen, H.L., Engberg, J., Ejlertsen, T., Bucker, R. and Nielsen, H. (2012) Short-term and medium-term clinical outcomes of *Campylobacter concisus* infection. Clin. Microbiol. Infect. 18, E459–E465.
[19] Kaakoush, N.O., Deshpande, N.P., Wilkins, M.R., Tan, C.G., Burgos-Portugal, J.A., Raftery, M.J., Day, A.S., Lemberg, D.A. and Mitchell, H. (2011) The pathogenic potential of *Campylobacter concisus* strains associated with chronic intestinal diseases. PLoS One 6, e29045.
[20] Man, S.M., Kaakoush, N.O., Leach, S.T., Nahidi, L., Lu, H.K., Norman, J., Day, A.S., Zhang, L. and Mitchell, H.M. (2010) Host attachment, invasion, and stimulation of proinflammatory cytokines by *Campylobacter concisus* and other non-*Campylobacter jejuni Campylobacter* species. J. Infect. Dis. 202, 1855–1865.
[21] Deshpande, N.P., Kaakoush, N.O., Wilkins, M.R. and Mitchell, H.M. (2013) Comparative genomics of *Campylobacter concisus* isolates reveals genetic diversity and provides insights into disease association. BMC Genomics 14, 585.
[22] Lapaquette, P., Glasser, A.L., Huett, A., Xavier, R.J. and Darfeuille-Michaud, A. (2010) Crohn's disease-associated adherent-invasive *E. coli* are selectively favoured by impaired autophagy to replicate intracellularly. Cell Microbiol. 12, 99–113.
[23] Man, S.M., Kaakoush, N.O. and Mitchell, H.M. (2011) The role of bacteria and pattern-recognition receptors in Crohn's disease. Nat. Rev. Gastroenterol. Hepatol. 8, 152–168.
[24] McCarroll, S.A., Huett, A., Kuballa, P., Chilewski, S.D., Landry, A., Goyette, P., Zody, M.C., Hall, J.L., Brant, S.R., Cho, J.H., Duerr, R.H., Silverberg, M.S., Taylor, K.D., Rioux, J.D., Altshuler, D., Daly, M.J. and Xavier, R.J. (2008) Deletion polymorphism upstream of IRGM associated with altered IRGM expression and Crohn's disease. Nat. Genet. 40, 1107–1112.
[25] Singh, S.B., Davis, A.S., Taylor, G.A. and Deretic, V. (2006) Human IRGM induces autophagy to eliminate intracellular mycobacteria. Science 313, 1438–1441.
[26] Everest, P.H., Goossens, H., Butzler, J.P., Lloyd, D., Knutton, S., Ketley, J.M. and Williams, P.H. (1992) Differentiated Caco-2 cells as a model for enteric invasion by *Campylobacter jejuni* and *C. coli*. J. Med. Microbiol. 37, 319–325.
[27] Wu, Y.T., Tan, H.L., Shui, G., Bauvy, C., Huang, Q., Wenk, M.R., Ong, C.N., Codogno, P. and Shen, H.M. (2010) Dual role of 3-methyladenine in modulation of autophagy via different temporal patterns of inhibition on class I and III phosphoinositide 3-kinase. J. Biol. Chem. 285, 10850–10861.
[28] Cloonan, S., Voldman, A., Weitz, A., Blaser, M., Iovine, N. and Cloonan, S.J. (2008) Autophagy and the innate immune response to *Campylobacter jejuni*. Clin. Infect. Dis., B3797.
[29] Yuan, K., Huang, C., Fox, J., Laturnus, D., Carlson, E., Zhang, B., Yin, Q., Gao, H. and Wu, M. (2012) Autophagy plays an essential role in the clearance of *Pseudomonas aeruginosa* by alveolar macrophages. J. Cell Sci. 125, 507–515.
[30] Wang, Y.H., Wu, J.J. and Lei, H.Y. (2009) The autophagic induction in *Helicobacter pylori*-infected macrophage. Exp. Biol. Med. 234, 171–180.
[31] Barth, S., Glick, D. and Macleod, K.F. (2010) Autophagy: assays and artifacts. J. Pathol. 221, 117–124.
[32] Oelschlaeger, T.A., Guerry, P. and Kopecko, D.J. (1993) Unusual microtubule-dependent endocytosis mechanisms triggered by *Campylobacter jejuni* and *Citrobacter freundii*. Proc. Natl. Acad. Sci. U.S.A. 90, 6884–6888.
[33] Fan, C., Wang, W., Zhao, B., Zhang, S. and Miao, J. (2006) Chloroquine inhibits cell growth and induces cell death in A549 lung cancer cells. Bioorg. Med. Chem. 14, 3218–3222.
[34] Lam, G.Y., Cemma, M., Muise, A.M., Higgins, D.E. and Brumell, J.H. (2013) Host and bacterial factors that regulate LC3 recruitment to *Listeria monocytogenes* during the early stages of macrophage infection. Autophagy 9, 1–11.
[35] Guerry, P. and Szymanski, C.M. (2008) *Campylobacter* sugars sticking out. Trends Microbiol. 16, 428–435.
[36] Bouwman, L.I., Niewold, P. and van Putten, J.P. (2013) Basolateral invasion and trafficking of *Campylobacter jejuni* in polarized epithelial cells. PLoS One 8, e54759.
[37] Lee, E.W., Seo, J., Jeong, M., Lee, S. and Song, J. (2012) The roles of FADD in extrinsic apoptosis and necroptosis. BMB Rep. 45, 496–508.
[38] Oltvai, Z.N., Milliman, C.L. and Korsmeyer, S.J. (1993) Bcl-2 heterodimerizes *in vivo* with a conserved homolog, Bax, that accelerates programmed cell death. Cell 74, 609–619.
[39] Hocker, R., Walker, A. and Schmitz, I. (2013) Inhibition of autophagy through MAPK14-mediated phosphorylation of ATG5. Autophagy 9, 426–428.
[40] Jia, G., Cheng, G., Gangahar, D.M. and Agrawal, D.K. (2006) Insulin-like growth factor-1 and TNF-alpha regulate autophagy through c-jun N-terminal kinase and Akt pathways in human atherosclerotic vascular smooth cells. Immunol. Cell Biol. 84, 448–454.
[41] Moresi, V., Carrer, M., Grueter, C.E., Rifki, O.F., Shelton, J.M., Richardson, J.A., Bassel-Duby, R. and Olson, E.N. (2012) Histone deacetylases 1 and 2 regulate autophagy flux and skeletal muscle homeostasis in mice. Proc. Natl. Acad. Sci. U.S.A. 109, 1649–1654.
[42] Tanida, I. (2011) Autophagy basics. Microbiol. Immunol. 55, 1–11.
[43] Pan, L., Li, Y., Jia, L., Qin, Y., Qi, G., Cheng, J., Qi, Y., Li, H. and Du, J. (2012) Cathepsin S deficiency results in abnormal accumulation of autophagosomes in macrophages and enhances Ang II-induced cardiac inflammation. PLoS One 7, e35315.
[44] Tatti, M., Motta, M., Di Bartolomeo, S., Cianfanelli, V. and Salvioli, R. (2013) Cathepsin-mediated regulation of autophagy in saposin C deficiency. Autophagy 9, 241–243.
[45] Rioux, J.D., Xavier, R.J., Taylor, K.D., Silverberg, M.S., Goyette, P., Huett, A., Green, T., Kuballa, P., Barmada, M.M., Datta, L.W., Shugart, Y.Y., Griffiths, A.M., Targan, S.R., Ippoliti, A.F., Bernard, E.J., Mei, L., Nicolae, D.L., Regueiro, M., Schumm, L.P., Steinhart, A.H., Rotter, J.I., Duerr, R.H., Cho, J.H., Daly, M.J. and Brant, S.R. (2007) Genome-wide association study identifies new susceptibility loci for Crohn disease and implicates autophagy in disease pathogenesis. Nat. Genet. 39, 596–604.
[46] Ravikumar, B., Sarkar, S., Davies, J.E., Futter, M., Garcia-Arencibia, M., Green-Thompson, Z.W., Jimenez-Sanchez, M., Korolchuk, V.I., Lichtenberg, M., Luo, S., Massey, D.C., Menzies, F.M., Moreau, K., Narayanan, U., Renna, M., Siddiqi, F.H., Underwood, B.R., Winslow, A.R. and Rubinsztein, D.C. (2010) Regulation of mammalian autophagy in physiology and pathophysiology. Physiol. Rev. 90, 1383–1435.